Unusual anti-leukaemia activity of nanoformulated naproxen and other non-steroidal anti-inflammatory drugs

Raj Kumar[a, b], Prem Felix Siril[a, b] *, Farideh Javid[c]

[a] School of Basic Sciences, Indian Institute of Technology Mandi, Mandi, Himachal Pradesh, India-175005.

[b] Advanced Material Research Centre, Indian Institute of Technology Mandi, Mandi, Himachal Pradesh, India-175005.

[c] School of Applied Science, University of Huddersfield, Queensgate, Huddersfield, United Kingdom-HD1 3DH.

[*] Corresponding author: Dr. Prem Felix Siril

Postal Address:

Dr. Prem Felix Siril, School of Basic Sciences, Indian Institute of Technology Mandi, Mandi-175005, India

Telephone: +91-1905267040, Fax: +91-1905-237942

Email Address: (Dr. Prem Felix Siril: prem@iitmandi.ac.in)

Abstract

The non-steroidal anti-inflammatory drugs (NSAIDs) are the most widely used pharmaceuticals worldwide. Interestingly, many of them have significant anticancer properties too. However, the poor water solubility of certain NSAIDs limits their application for cancer treatment. Nanosizing of such drugs can help to improve the solubility and this may result in enhanced anticancer activities too. Moreover, over dosages and the accompanying side effects of NSAIDs can be minimized by improving their solubility and bioavailability. Successful nanoformulation of three NSAIDs: ibuprofen (IBP), ketoprufen (KP) and naproxen (NAP) using a novel evaporation assisted solvent-antisolvent interaction (EASAI) method is reported here. Three water soluble and biocompatible polymers: polyvinylpyrrolidone (PVP), polyvinyl alcohol (PVA) and hydroxypropyl methylcellulose (HPMC) were used to stabilize the drug nanoparticles. Particles having spherical morphology with average size below 30 nm were thoroughly characterized using dynamic light scattering and field emission scanning electron microscopy (FESEM) imaging. The nanoformulation resulted in ten to fifteen fold improvements in the solubility and significant enhancement in the in-vitro drug release profiles of the NSAIDs. Anticancer screening of the nanoformulated NSAIDs against five different cancer cell lines such as MCF-7 (Human breast cancer cell line), (Human pancreatic cancer cell line) MIA-PA-CA-2, (Human colon cancer cell line) HT-29, (Human leukemia cell line) Jurkat and (human ovarian carcinoma cell line) A2780 was performed. All the nanoformulated samples showed improved anticancer activity against the Leukemia cancer cell line, out of which NAP-PVP showed the highest anti-cancer activity. The anti-Leukemia activity of NAP-PVP was more than twice that of doxorubicin which is a standard anticancer drug.

1. Introduction

Non-steroidal anti-inflammatory drugs (NSAIDs) are the most frequently used medicines worldwide [1-3]. NSAIDs have effective anti-inflammatory, antipyretic and analgesic activities. Hence they are commonly used for treating various ailments such as pain, fever and inflammatory conditions including rheumatoid arthritis and osteoarthritis. Interestingly, they have a very long history, as 3500 years ago Greek physicians used extracts of willow bark and leaves to treat fever [4]. Later, Salicin, the active ingredient of willow bark was identified in the 17^{th} century [5]. Salicylic acid became commercially available in the year 1860 [6]. The mechanism of action of aspirin was discovered by John Vane in 1960 [7]. It seems that the glory of NSAIDs is here to stay as there have been several reports on the anticancer activities of NSAIDs. They were found to be effective against colorectal, colon, breast and pancreatic cancers [8-12]. However, their anticancer efficacy was poorer than the common anticancer drugs that are currently being used [13]. But, it has been proposed that the anticancer activities of many NSAIDs can be enhanced by proper formulation or derivatisation [14, 15]. This is mainly because; NSAIDs such as IBP, KP and NAP have poor bioavailability due to their poor solubility in water [16]. Higher doses of these drugs have to be administered for effective therapy. Oral administration of these drugs in such higher doses often leads to gastrointestinal toxicity, which is a major problem [17].

NSAIDs such as aspirin [18], indomethacin [19], celecoxib [20], IBP [21], KP [22] and NAP [23] have significant anticancer activities. However, there is scope to improve the anticancer activities of the NSAIDs. Different synthetic approaches were developed to enhance the anticancer activity of NSAIDs. For example, complex formation with metals (example Ru) and derivatisation (phospho-ibuprofen) was attempted to improve the solubility of IBP [24]. The advent of nanotechnology opened up a new window which can be used to increase the bioavailability and the anticancer activity of NSAIDs by reducing the particle size without changing their chemical structure. A number of nanoformulation techniques and drug delivery systems were developed for the delivery of active pharmaceutical ingredients in general [24]. Some attempts were made to nanoformulate NSAIDs also [25]. For example, delivery of IBP using micelles as carrier to breast cancer cells showed remarkable reduction in cancer cell viability [25]. Hydroxyapatite-chitosan nanocomposite was used for the delivery of celecoxib for the treatment of colon cancer [26]. KP loaded polymeric nanocapsules showed good anticancer activity against glioblastomamultiforme (GBM) [27]. The IBP loaded PLGA nanoparticles were prepared for the treatment of human gastric cancer (MKN45 cell) [28]. Nanoformulation of the NSAIDs using a novel evaporation assisted solvent antisolvent interaction method (EASAI) has been attempted in the present study. Here we report the significantly improved anti-cancer activities of nanoforumulated NSAIDs.

In fact, poor solubility of drugs in water is a wider issue and a major challenge for the pharmaceutical industry [29]. Drug discovery is a costly affair and yet about 40% of the newly synthesized drug molecules are having poor water solubility and hence low bioavailability [30]. There are number of ways by which bioavailability of drugs having poor water solubility can be enhanced [31]. Particle size reduction is a very effective way to enhance the solubility. Solubility of smaller particles is higher than bigger ones due to the enhanced surface area [32]. Nanosizing of drug particles has been proven to be a tangible option for achieving enhanced solubility [33]. Formulating drugs with water soluble polymers, surfactants, lipids and other excipient can also lead to enhanced solubility [34, 35]. EASAI method is an effective method for the preparation of both bare drug nanoparticles as well as polymer stabilized nanoparticles with average particle size well below 100 nm. In the EASAI method, the rate of precipitation is enhanced by using conditions favouring evaporation of the solvent [36].

All the three stabilizers (PVP, PVA and HPMC) are widely used in the nanoformulation of active pharmaceutical ingredients (APIs) [37]. One of the outstanding properties of these stabilizers is their universal solubility in hydrophilic and hydrophobic solvents [38]. They have good binding capacity, affinity to hydrophobic and hydrophilic surfaces and ability to form water soluble complexes [39]. PVA is mainly used in topical pharmaceutical and ophthalmic formulations [39]. PVA hydrogels have been used for various biomedical and pharmaceutical applications such as in the lining for artificial hearts and drug delivery [40]. HPMC is widely used in controlled drug release formulations [37, 39, 41]. PVP is also widely used in drug delivery systems and formulation of pharmaceutics [42-45]. All the polymers are easily accepted, the necessary doses are easy to formulate and approved by the U.S. Food and Drug Administration (FDA).

The prepared nanodrugs were tested for their anticancer activities in five different cancer cell lines: MCF-7 (Human breast cancer cell line), (Human pancreatic cancer cell line) MIA-PA-CA-2, (Human colon cancer cell line) HT-29, (Human leukemia cell line) Jurkat and (human ovarian carcinoma cell line) A2780. The efficacy of the nanodrugs was compared with doxorubicin having trade name adriamycine (ADR), which is a commonly used anticancer drug [46].

2. Materials and methods

2.1. Materials

IBP, KP and NAP, acetone, ethanol, HPMC (86,000), PVP (40,000), PVA (16,000) and phosphate buffer saline pH 7.4 were purchased from Sigma Aldrich and used as received. Average molecular weights of the polymers are given in parenthesis. HPLC micro syringe was purchased from Hamilton, USA. Syringe filters of 0.22 and 0.45 μm and Whatman®Anodisc 25 filter of 20 nm pore size with filtration setup were purchased from Millipore, USA. Ultra-pure water (18.2 MΩ-cm) from double stage water purifier (Elgapurelab option-R7) was used for all the experiments.

2.2. Preparation of NSAID nanoparticles

Stock solutions of 100 mM concentration were prepared by dissolving accurately weighed quantities of the drugs in acetone. Lower concentration solutions were prepared by diluting the stock solutions. The solutions were always filtered immediately prior to their use, through a 0.22 μm syringe filter membrane to remove any particles present in it. The antisolvent (25 ml) was heated to 70 °C in a 100 ml conical flask. The drug solution (100 μl) of known concentration was quickly injected to the hot antisolvent using a micro-syringe under magnetic stirring to precipitate nanoparticles. Stirring was continued up to few minutes after the injection. Aqueous solutions of the respective stabilizers were used as antisolvent to prepare NSAID-PVP, NSAID-PVA and NSAID-HPMC nanoparticles.

2.3. Characterization

Particles size (z-average diameter, d/nm), polydispersity index (PDI) and zeta potential of the precipitated nanoparticles was measured using DLS method (Zetasizer Nano ZS, Malvern Instrument Ltd., UK) at 25 °C. The instrument contains a 4 mW He–Ne laser operating at a wavelength of 633 nm and incorporates non-invasive backscatter optics (NIBS). All measurements were made at a detection angle of 173°. Particle size and morphology of the samples was studied by FESEM (Supra55 VP model, ZEISS) imaging. Suspensions of the nanoparticles were drop casted on glass slides and dried. The samples were then sputter coated with gold at 20 mA for 180 s before FESEM imaging. The particle sizes were measured manually from FESEM images using standard Image J software. FTIR spectroscopy was performed using the Perkin Elmer FTIR emission spectrometer (Spectrum Two) frequency range from 4000 to 600 cm^{-1} with a resolution of 4 cm^{-1} and 8 scans. The

samples were properly grounded with KBr powder and then pressed to obtain a suitably sized pellet for FTIR spectrum measurement. Pure KBr Pellet was used for background correction. Samples were placed in glass sample holders and XRD patterns were recorded in the 2θ range of 10 to 70 °C with scan rate of 2 °/min and step size of 0.02°. Smart Lab X-Ray Diffractometer (Rigaku, Japan) with Cu Kα radiation as X-ray source (λ = 0.15418 nm) at room temperature was used. The voltage and current applied were 45 kV and 100 mA respectively. DSC analyses were carried out using Netzsch STA 449 F1 Jupiter instrument by keeping 2-3 mg of samples in alumina crucible with a lid having pin hole at the middle. The samples were heated from room temperature to 500 °C at a heating rate of 5 °C/min under nitrogen atmosphere with a flow rate of 60 ml min^{-1}. An empty crucible was used as the reference.

2.4. Solubility, encapsulation efficiency (%EE) and in-vitro dissolution studies

A known excess quantity of the sample was dissolved in water (3 ml) in a 50 ml round bottom flask by keeping it in a water bath at 37±1 °C. The solution was magnetically stirred at 100 rpm for 24 h. The solution was then centrifuged and the supernatant was filtered using Whatman®anodisc 25 filter of pore size 20 nm to remove any undissolved particles. The filtered solution was diluted to the required concentration by adding known volumes of water. Relative concentrations of the raw-drug and the respective nanoformulated drugs in the solutions were determined by measuring the optical densities using Shimadzu double beam UV-Vis spectrophotometer.

Known quantity of sample was dissolved in ethanol (3 ml) to study the % EE. The solution was filtered through Whatman®anodisc 25 filter having pore size 20 nm to remove all particles present in it. The %EE was calculated by measuring the amount of drug present in the solution. Absorption spectrum of the solution was recorded using UV visible spectrometer. The concentration of the drug that was dissolved in ethanol was found out from a previously generated calibration curve by serial dilution of a standard solution. The %EE was calculated using the following formula:

$$\% EE = \frac{Weight\ of\ the\ drug\ dissolved\ in\ ethanol}{Total\ weight\ of\ the\ drug\ added\ initially} X\ 100$$

The drug release profile of samples was tested using a USP microprocessor dissolution test apparatus, Model 1912 of Electronics India. The dissolution test was performed in 900 ml phosphate buffer saline medium (PH 7.4) at 37±1 °C and 100 rpm by adding 50 mg of sample. Aliquots of 2 ml were withdrawn at specified time intervals and replaced with fresh medium to maintain sink conditions. The withdrawn aliquots were centrifuged at 12000 rpm for 20 min and filtered using Whatman®Anodisc 25, filter of pore size 20 nm and the absorption spectra were recorded.

2.5. Cell culture and SRB assay

Anticancer activities of all the three raw NSAIDs, the respective nanoformulated NSAID nanoparticles (bare and polymer stabilized) and pure polymeric stabilizers were screened. The anticancer activities of the samples were studied by SRB and MTT assay [47-49]. The five different cell lines were maintained in ideal laboratory conditions. Human breast cancer cell line MCF7, human pancreatic cancer cell line MIA-PA-CA-2, human colon cancer cell lines HT-29, human leukemia cell line Jurkat and human ovarian carcinoma cell line A2780 were grown in tissue culture flasks in growth medium (RPMI-1640 with 2 mM L-glutamine, P^H 7.4, 10% fetal calf serum, 100 µg/ml streptomycin, and 100 units/ml penicillin) at 37 °C under the atmosphere of 5% CO_2 and 95% relative humidity by employing a CO_2 incubator. The cells at sub confluent stage were harvested from the flask by treatment with Trypsin (0.05% Trypsin in PBS containing 0.02% EDTA) and placed in growth medium [1]. The cells with more than 97% viability (trypan blue exclusion) were used for cytotoxicity studies. Aliquots of 100 µl of cells (density of cell 5 x 10^3 cell/well) were transferred to a well of 96-well tissue culture plate. The cells were allowed to grow for one day at 37 °C in a CO_2 incubator as mentioned above. The test materials at different concentrations were then added to the wells and cells were further allowed to grow for 48 h. Suitable blanks and positive controls were also included. Each test was performed in triplicate. The cell growth was stopped by gently layering 50 µl of 50% trichloroaceticacid (TCA) [1]. The plates were incubated at 4 °C for an hour to fix the cells attached to the bottom of the wells. Liquids of all the wells were gently pipetted out and discarded. The plates were air dried after washing five times with doubly distilled water to remove TCA, growth medium and other chemicals. 100 µL of SRB solution (0.4% in 1% acetic acid) was added to each well and the plates were incubated at ambient temperature for half an hour. The unbound SRB was quickly removed by washing the wells five times with 1% acetic acid. Plates were air dried, tris-buffer (100 µl of 0.01 M, pH 10.4) was added to all the wells and plates were gently stirred for 5 min on a mechanical stirrer [1]. The optical density was measured on ELISA reader at 540 nm. The cell growth in absence of any drug was considered 100% and in turn growth inhibition was calculated. GI50, TGI and LC50 values were determined by regression analysis [1, 50, 51]. The MTT assay was used for checking the anti-proliferative effects of the nanoformulated NSAIDs on A2780. In such experiments A2780 cell lines were maintained as monolayer culture in 75 ml flasks with 20 ml of complete media containing RPMI 1640, 10% FBS, 1% penicillin and streptomycin, 1% sodium Pyruvate and 1% 2Mm L-glutamine, incubated at 37C with 5% CO_2. A2780 were seeded in round bottom 96-well plates at 2500 cells/ mL concentration. Plates were incubated at 37 °C and 5% CO_2 for 24 h. After incubation the varying doses of the samples were added to 96-well plate. Plates were further incubated for 96 h. MTT assay (2,5-diphenyltetrazolium bromide) was performed at respective time point by addition of 200 µL/ well MTT, after 4 h incubation MTT was replaced with 150 µL/well DMSO. The absorption values were read at 540 nm.

3. Results and discussion

In the EASAI method, quick injection of drug solutions into hot antisolvent resulted in the evaporation of acetone and precipitation of nanoparticles as shown in Figure 1. Stirring was

continued for few minutes after the injection to yield smaller particles with narrow size distribution [52]. Nucleation occurs at the interphase between the droplets of the solution and the antisolvent (water). Accelerated nucleation takes place in EASAI due to evaporation of solvent and mixing with the antisolvent. The polymers those are present in the antisolvent bind on the surface of the drug particles immediately after nucleation, thus preventing further growth by acting as a barrier for the diffusion of drug molecules from the solution towards the nuclei and also by preventing particle agglomeration.

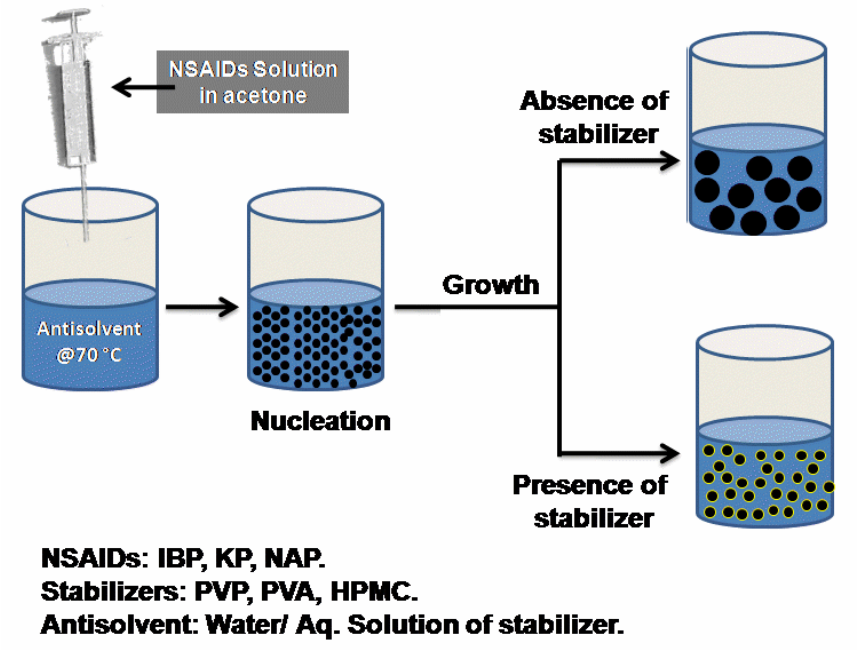

Figure 1 Schematic representation of the mechanism of nanoparticle formation in the EASAI method.

Antisolvent assisted precipitation is a very simple method. But, a number of experimental factors such as temperature of the antisolvent, concentration of the solution, rate of injection, nozzle geometry, ratio of solvent to antisolvent and ultrasonication affect the particle size and morphology of the nanoparticles [52]. Most of the experimental parameters that are required for the formation of smaller particles were optimized in one of our previous studies [52]. The previously optimized experimental parameters were used in the present study as the solvent (acetone)-antisolvent (water) pair was the same. It was observed that smaller particles were formed with solvent to antisolvent ratio of 1:250, at 70 °C [53]. This is because acetone having a boiling point of 56 °C evaporates at this temperature and evaporation assisted solvent-antisolvent interaction leads to smaller particle size, irrespective of the solute being precipitated [36, 53]. Similarly, the effect of ratio of solvent to antisolvent on particle size also may not change for the same pair of solvent and antisolvent. However, the effect of concentration of drug in its solution and the concentration of stabilizers (PVP, PVA & HPMC) on particles size was studied and the results are presented in the following sections.

3.1. Effect of drug concentration

The effect of drug concentration on particle size was studied by varying the drug concentration from 5-100 mM for all the three NSAIDs. The particle sizes that were measured using DLS are presented in Table 1. From the Table 1, it is clear that the particle size increases with increasing drug concentration. The size of IBP, KP and NAP particles, as per the DLS data, increased from 187±09, 197±12 and 220±18 to 394±28, 313±80 and 282±14 nm respectively, when concentration of the drugs in solution was increased from 5 to 100 mM. The increase in the particle size with increasing concentration can be explained based on the increased availability of solute molecules for particle growth after nucleation [53]. Nucleation occurs at the interface between antisolvent and solvent droplets in the antisolvent precipitation process. We have injected solutions of different drug concentrations at a fixed volume of solution and the antisolvent. Hence, the number nuclei formed initially could be similar, irrespective of the concentration. There is adequate supply of drug molecules in the solution for the prolonged growth of the nuclei to form larger particles, when the concentration of drug is more.

Table 1 Effect of drug concentration on the particle size of precipitated nanoparticles.

S. No.	Drug	Particles size (d/nm) measured using DLS			
		5 mM	25 mM	50 mM	100 mM
1	IBP	187±09	192±08	229±17	394±28
2	KP	197±12	216±10	219±05	313±80
3	NAP	220±18	223±18	274±16	282±14

3.2. The effect of different stabilizers and their concentrations on particle sizes

Three different polymeric stabilizers were used to inhibit the growth of drug nanoparticles and encapsulate them. The nature of the polymer and its concentration can affect the particle size [54]. The z-average particle sizes that were measured using DLS, when different polymers were used at varying concentrations to stabilize the particle sizes are given in Table 2. The concentration of polymeric stabilizers was optimized using 100 mM solutions of each drug. It is clearly evident from Table 2 that the particle sizes of the drug nanoparticles were influenced by the presence of polymeric stabilizers in the antisolvent. A number of interesting trends could be observed. There was variation in particle size with change in concentration of the polymers. Particle size was lowest when the concentration of PVP, PVA and HPMC was 0.2, 0.5 and 0.1 % (w/v) in the antisolvent respectively. Concentrations above and below these optimum values led to enhancement of particle sizes. Stabilizers control the particle size by getting adsorbed on the particle surfaces and by preventing aggregation. There may not be enough polymer molecules available to form at least a monolayer over the particles at lower concentrations [54]. This lack of availability of sufficient amount of stabilizers to control the growth of the particles resulted in larger particles [54]. At higher than optimum concentrations of the polymers, increase in osmotic pressure leads to increased attraction among colloidal particles leading to agglomeration [55]. When the concentration of stabilizers was optimum, the particle growth was controlled by stabilizers resulting in smaller particles. The drug nanoparticles prepared with the optimized stabilizer concentrations were

further characterized thoroughly. Drug nanoparticles prepared in presence of the polymers have been denoted as NSAID-stabilizer (for example, IBP-PVP, IBP-HPMC, IBP-PVA etc.).The pure drug nanoparticles have been denoted as nano-IBP, nano-KP and nano-NAP respectively.

Table 2 Effect of different stabilizers and their varying concentrations on the z-average particle size of different NSAIDs. All the particles were prepared by injecting solutions of the drugs in acetone (100 µl, 100 mM) to aqueous solution of the polymers (25 ml) at 70 °C.

	Particle size (d/nm) measured using DLS								
%(w/v)	**IBUPROFEN (IBP)**			**KETOPROFEN (KP)**			**NAPROXEN (NAP)**		
	PVP	**PVA**	**HPMC**	**PVP**	**PVA**	**HPMC**	**PVP**	**PVA**	**HPMC**
0.05	268±12	982±47	252±19	414±21	712±63	243±09	319±13	719±40	303±05
0.1	198±14	515±41	**86±15**	369±14	653±21	**156±08**	237±06	491±52	**101±37**
0.15	132±09	452±23	237±31	212±23	524±47	247±15	208±09	331±33	189±11
0.2	**43±14**	390±31	404±28	**173±15**	421±45	401±13	**113±07**	241±41	273±32
0.3	210±17	287±17	656±17	229±18	343±18	565±42	167±18	179±32	397±21
0.4	389±12	145±25	789±62	282±26	278±31	706±55	271±19	122±29	435±59
0.5	611±20	**90±43**	821±44	499±22	**204±19**	894±34	341±23	**70±28**	676±45
0.6	743±39	271±58	963±42	756±52	349±37	976±59	539±27	199±20	819±44

It can also be seen from Table 2 that the apparent effect of stabilizers on the particle size varied with the nature of stabilizers as well as the drug. PVP, HPMC and PVA were the most effective stabilizer for IBP, KP and NAP nanoparticles, respectively. Zeta potentials of the formulated drug nanoparticles are given in Table T1 (electronic supporting information). Evidently, the zeta potentials of bare drug nanoparticles were negative and the actual values varied with particle sizes as well as the nature of each drug. KP and IBP nanoparticles had strongly negative zeta potential. NAP nanoparticles have zeta potential closer to zero. Smaller particles have more negative zeta potentials and the values gradually became less negative with increase in particle sizes. However, zeta potential values became closer to zero (-1.0 to -5.5 mV) after stabilization with the polymers. When electrostatic stabilization mechanism is operating, colloidal suspension of particles with zeta potential values greater than ±30 mV is generally considered to be stable. As the charge on polymer stabilized drug nanoparticles is close to zero in the present nanoformulation, stabilization by the polymers seems to be purely steric in nature. Stability of particles against Ostwald ripening was checked by measuring the

particle size of the aqueous suspensions after six months. Mild sonication for 10 min was found to be sufficient for the re-dispersal of particle agglomerates, even after six months.

DLS being an indirect method for characterizing the particle sizes, FESEM imaging was done to characterize the particle properties including size. Some representative FESEM images of the bare as well as polymer stabilized nanoparticles of IBP, KP and NAP are given in Figure 2, Figure 3 and Figure 4 respectively. Particle sizes were calculated from the FESEM images and are summarized in Table 3. Particle sizes that were measured using DLS also are given in Table 3 for direct comparison. The Z-average particle sizes those are measured by DLS were always higher than the actual particle sizes those were measured from FESEM images. This is obvious as DLS indirectly measures hydrodynamic radius whereas diameters of dried particles are directly measured from the FESEM images. Such difference in particle size that is measured using DLS and FESEM is widely reported in the literature [56]. From Table 3, it is clear that the particle sizes were higher for bare drug nanoparticles. However, the average particle size of all the NSAID particles decreased to less than 30 nm in presence of the polymeric stabilizers. Morphology of the drug nanoparticles was spherical in presence and absence of the polymeric stabilizers. The particles were observed to be well dispersed without any aggregation in FESEM images.

Table 3 Particle sizes of the nano-NSAIDs and NSAID-stabilizer nanoparticles that were measured using DLS and FESEM. Bare drug nanoparticles were prepared by injecting solutions of the drug in acetone (100 μl, 100 mM) to water (25 ml) at 70 °C. Polymer stabilized nanoparticles were formed when the antisolvent (water) contained optimized concentrations of PVP (0.2% w/v), PVA (0.5% w/v) and HPMC (0.1% w/v).

S.No	Drug	Particle size (d/nm) measured using DLS			
		Nano	PVP	PVA	HPMC
1	IBP	394±28	43±14	90±43	86±15
2	KP	313±80	173±15	204±19	156±08
3	NAP	282±14	113±07	70±28	101±37
		Particle size (d/nm) measured using FESEM			
4	IBP	127±41	23±07	25±06	27±04
5	KP	81±17	24±04	22±04	21±06
6	NAP	162±42	21±03	28±04	23±04

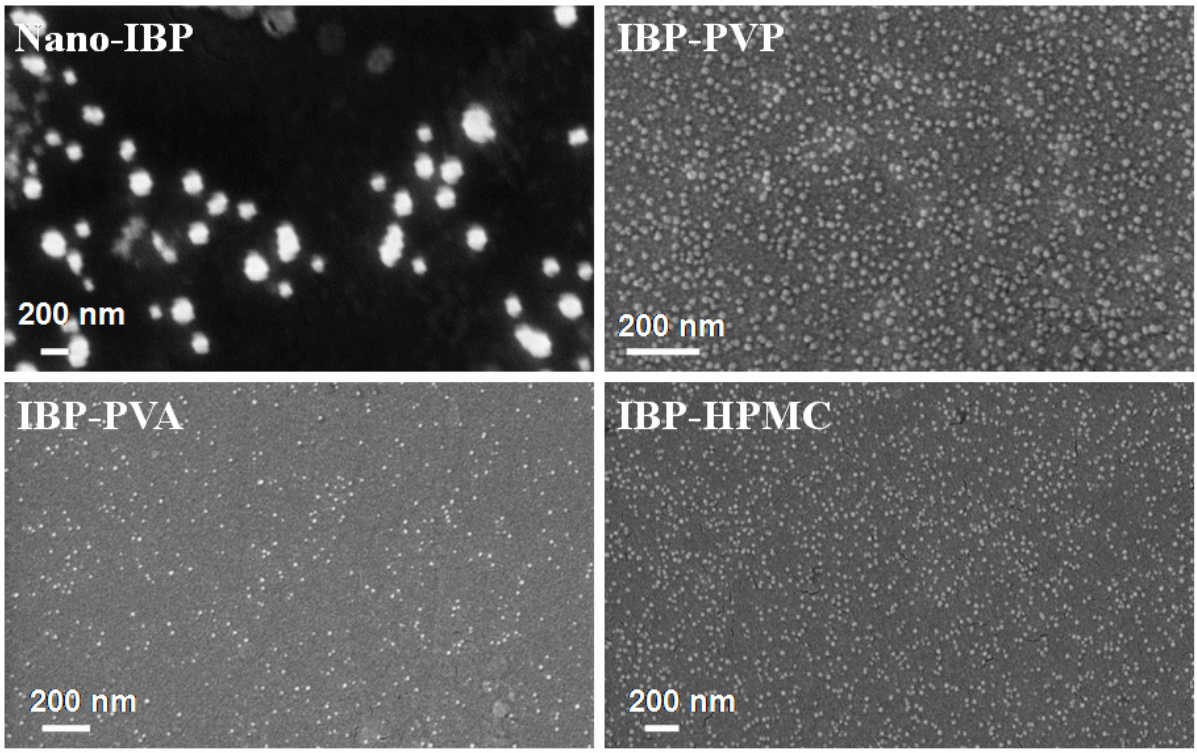

Figure 2 Representative FESEM images of the nanoparticles of IBP.

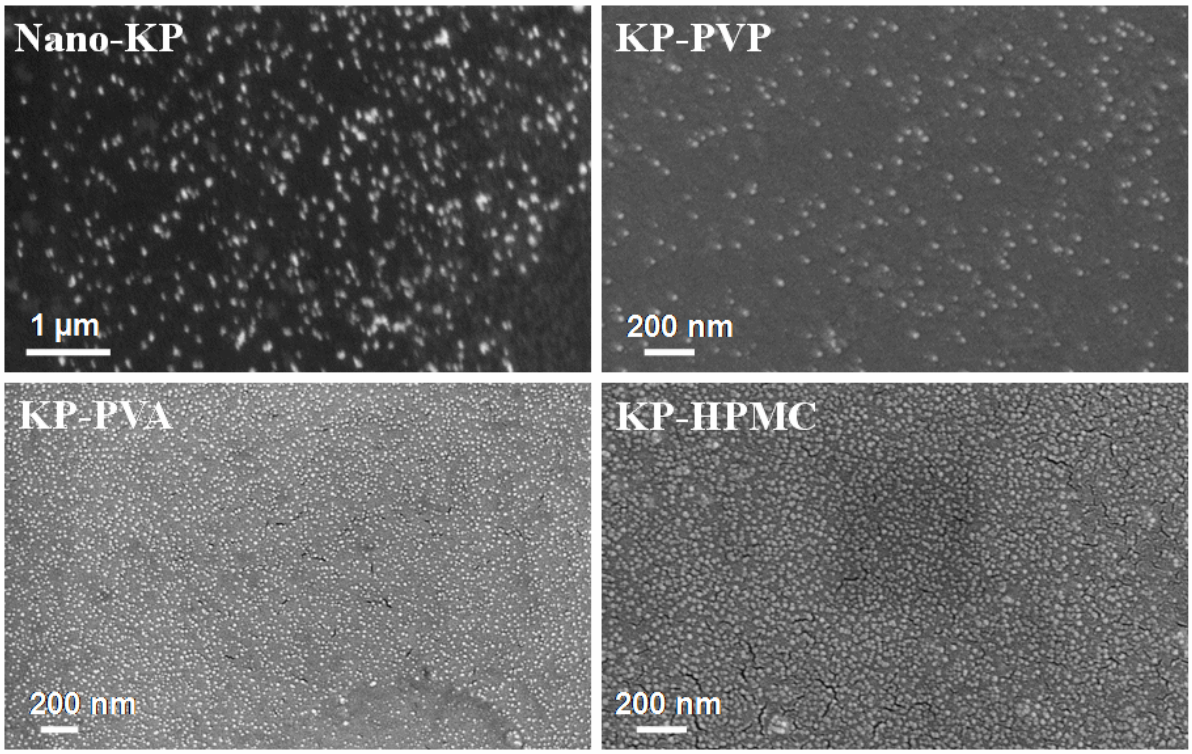

Figure 3 Representative FESEM images of the nanoparticles of KP.

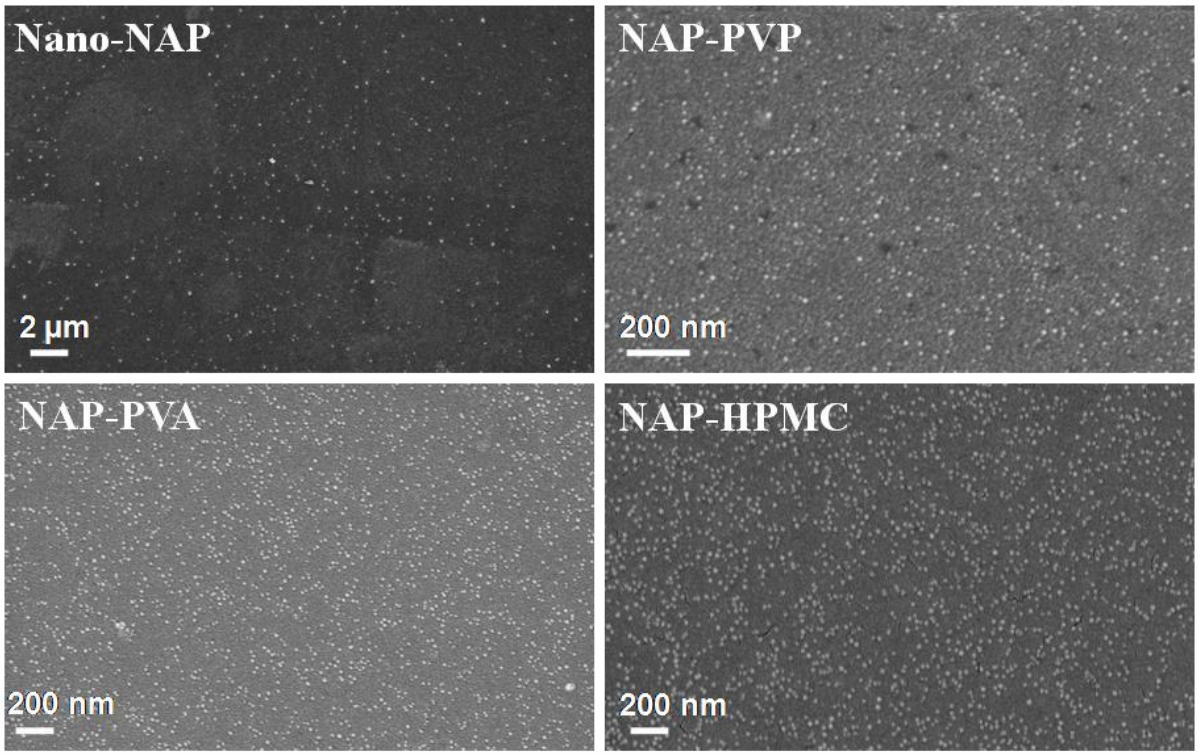

Figure 4 Representative FESEM images of the nanoparticles of NAP.

Chemical, crystallographic, thermal and solubility characteristics of nano-NSAIDs and NSAID-polymer nanoparticles were characterized thoroughly and compared with the raw-NSAIDs and the details are presented in the following sections.

3.3. Infrared spectroscopy

FTIR spectra of all the samples are reported in Figures S1 (electronic supporting information). A summary of the characteristic FTIR peaks for each drug are presented in Table T2 (electronic supporting information). The characteristic bands for all the prepared nano-NSAIDs matched well with the corresponding raw-drugs and the literature reports also [57]. No peak shift was observed for any of the prepared nanodrugs, irrespective of the drug and stabilizer that were used. Thus, chemical interaction between drug and stabilizers can be ruled out. The interaction between the stabilizers and the drugs seem to be of the weak Van der waal's type.

3.4. X-ray diffraction

XRD patterns for all the three raw-drugs and their nanoparticles are presented in Figure S2 (electronic supporting information). The characteristic XRD peaks for each drug are presented in Table T3 (electronic supporting information). The XRD patterns of the nanoformulated drugs matched well with the XRD patterns of raw-drugs. There was good agreement of the patterns with the literature reports also [58-60]. There was no change in crystal structure on nanoformulation as the peak positions of the raw-drugs and the nanoparticles matched very well. It indicates that the polymorphic forms are the same in the

nanoformulated NSAIDs and the corresponding raw-drugs. However, the relative intensities of various peaks in XRD patterns were different. Relative abundance of the planes exposed to the X-rays would have been altered; producing the variation in relative intensities of the peaks [61]. Such crystal habit modifications are possible due to the variation of particle sizes [61].

3.5. Thermal characteristics

Overlays of DSC thermal curves for all the prepared samples along with raw-drugs are presented in Figure S3 (electronic supporting information). The corresponding phenomenological data is summarized in Table T4 (electronic supporting information). A single endothermic event was observed in each of the thermal curves for all the three drugs and their nanoparticles. This endothermic event corresponds to melting of the drugs. The melting point of raw-NSAIDs matched well with the data that is reported in the literature [62-64]. The nanoformulated NSAIDs also had somewhat similar melting points as the raw-NSAIDs. Slight lowering of the melting points was observed in most cases while the lowering in melting point was considerable for KP-PVA and KP-PVP.

Relative crystallinity of the nano-NSAID particles were calculated by comparing the enthalpy of melting as measured by DSC with the corresponding raw-drug. The calculated % crystallinity data are also reported in Table T4 (electronic supporting information). The nanoformulated drug samples had relatively lower crystallinity compared to their raw-counterparts. This can be explained based on the decrease in particle size and increase in amorphous content. However, relative crystallinity was more than 90 % for most of the nanoformulated NSAIDs.

3.6. Solubility

The prepared nano-NSAIDs showed enhanced solubility compared to raw-NSAIDs. The polymer supported drug nanoparticles showed higher solubility than the nano-drugs. The relative solubility of prepared nanoparticles was calculated by considering the solubility of the most soluble sample to be equal to“1” for each drug. The relative solubility values are summarized in Tables T5 (electronic supporting information). The solubility of raw-IBP and its nanoparticles were in the following order: IBP-HPMC > IBP-PVA > IBP-PVP > Nano-IBP > Raw-IBP. Similar trend was observed for NAP also. But the solubility trend for KP was different compared to NAP and IBP. The trend was in the following order: KP-PVA > KP-HPMC > KP-PVP > Nano-KP > Raw-KP. Enhancement in the solubility of prepared samples compared to raw-drug is mainly due to the enhanced surface area as the solubility increased with decrease in particle size. Increased presence of amorphous content in the nanoparticles also could be a reason for enhancement in solubility [57].

3.7. In-vitro drug release studies

The in-vitro drug release profiles of all the prepared drug nanoparticles along with raw-drugs are shown in Figure 5. The % drug release after 180 min from the nanoformulated drugs is higher than the corresponding raw-drugs, irrespective of the drug that was used. Initial burst release was observed followed by an induction period and subsequent enhanced release rate was a common feature for all the three raw-NSAIDs. About 60 % of the drug molecules were released from all the three raw-NSAIDs after 180 min. The drug release profile of bare nanoparticles also followed a similar profile to the raw-drugs. Albeit, the final % of the drug released after 180 min from the bare nanoparticles was higher than their raw-counterparts. The drug release profiles of the polymer stabilized nanoparticles were significantly different from raw and bare nano drugs in most cases. About 80 -100 % of the drug was released from the polymer-NSAID nanoparticles within 120 min. Among the polymers, HPMC seems to be the most efficient in enhancing the dissolution of the drugs. 100 % drug release was observed for all the three NSAID-HPMC nanoparticles at 180 min. A somewhat controlled release profile was observed in IBP and KP when they were nanoformulated using PVP. A similar controlled release profile was observed for NAP nanoparticles, but in presence of PVA. The observed drug release profiles could be due to interplay between the amounts of amorphous content in the nanoformulated drugs and the solubilizing ability of the polymers. Overall, increase in the rate of drug release from nano-sized particles is mainly due to the decrease in particles size and increase in surface area.

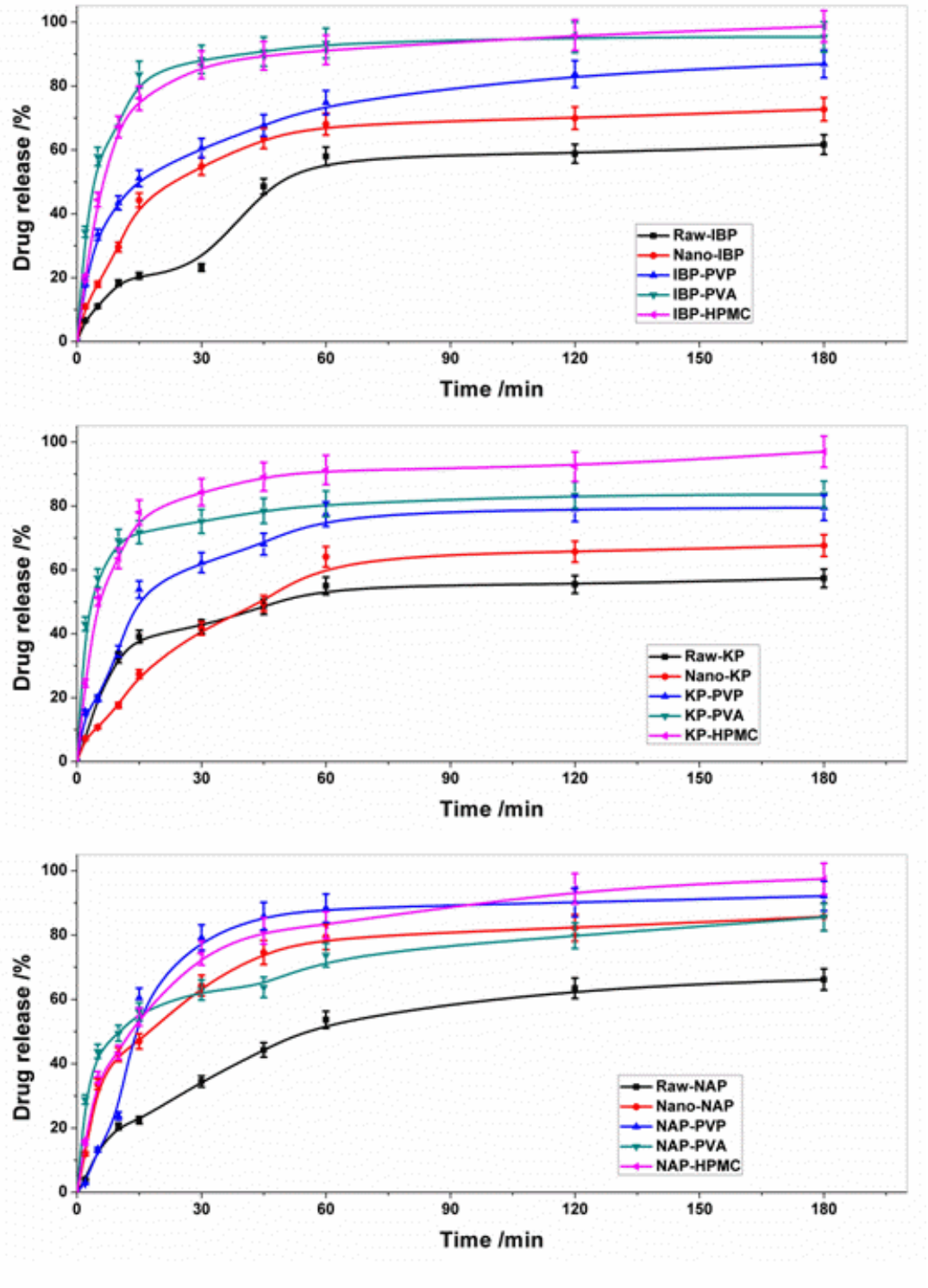

Figure 5 In-vitro drug release profiles of raw-NSAIDs and their nanoformulated samples

3.8. Anticancer activity

The anticancer activities of the raw-NSAIDs, raw-polymers and the nanoformulated NSAIDs were studied and compared with doxorubicine (ADR). The anticancer activity data on four cancer cell lines are presented in Table T5 (electronic supporting information). It is clearly

evident from the data that most of the nanoformulated NSAIDs showed very good anticancer activity against leukemia cancer cell line. Unfortunately, they have very poor anticancer activity against other studied cancer cell lines in comparison to the standard drug. Among, the NSAIDs, NAP samples showed better anti-leukemia activity when compared to IBP and KP samples. Interestingly, even the raw-NAP showed fairly good anti-leukemia activity. The GI50 values of NAP-HPMC and NAP-PVP were considerably lower than that for Doxorubicin. The plot of % viability of Jurkat cells against varying concentrations of the raw-NSAIDS and nanoformulated NSAIDs are shown in Figure 6 along with the data for the standard anticancer drug. The results for other cell lines are shown in Figure S4 (electronic supporting information). Nanoformulated NAP showed some anti-cancer activity against MCF-7 (Human breast cancer cell line) also. Excellent anti-leukaemia activity of NAP-HPMC and NAP-PVP was evident at all concentrations as their activity was better than the standard drug. Almost 100 % cell death could be achieved by using NAP-PVP at a concentration of 80 μg/ml (347.8 μM). 50% cell death was observed for very low concentrations such as 20.1 μg/ml (87.3 μM) and 37.0 μg/ml (160.8 μM) for NAP-PVP and NAP-HPMC respectively. Whereas, doxorubicin showed 50 % cell viability at a concentration of 45.1 μg/ml (196 μM). Thus, the activity of NAP-PVP was more than two times better than the standard drug.

In general, the GI50 value should be less than 10 μM for a candidate drug molecule to be considered as anticancer drug [65]. This is mainly because chemotherapeutics for anticancer treatment are highly toxic to normal cells and this leads to a number of side effects. However NAP is an FDA approved NSAID that is available off the shelf and has been in vogue in the market for quite some time. Administration of two commercially available NAP tablets (500 mg) per day with 12 h gap is already approved. Thus, the stringent low GI50 values of anticancer drugs need not be applied to NSAIDs for anticancer therapy.

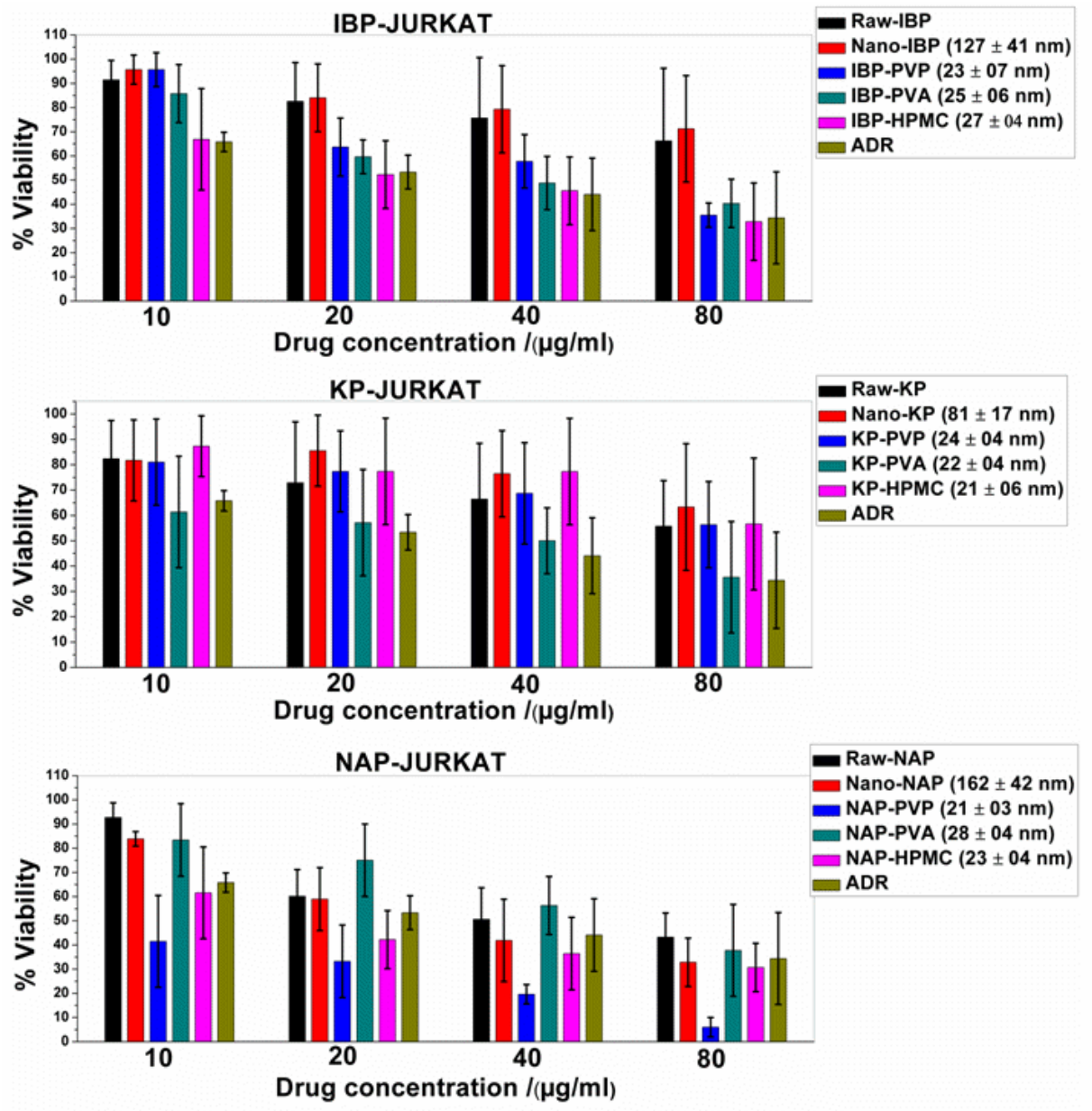

Figure 6 Plots of % cell viability of human leukemia cells (Jurkat) against varying concentrations of raw and nanoformulated NSAIDs. Average particle size of the nanoformulated NSAIDs that were measured from FESEM images are mentioned along with respective samples.

Enhancement in anticancer activity of NAP by the nanoformulation is clearly evident from the data and this must be mainly due to enhancement in solubility. Anticancer activity of NAP was reported with IC_{50} value of 1150 μM on HT-29 colon tumor cells with 72 h of treatment [66]. However, the IC_{50} value for NAP was very low in a number of human cancer cell lines when it was incubated after dissolving in dimethyl sulfoxide (DMSO) [67]. Thus solubility appears to be a key factor in the anticancer activity of NAP. However, it was not possible to correlate the anticancer activity with the solubility alone among the nanoformulated NAP samples in the present work. Apart from improvements in solubility,

derivatization of NAP also is known to enhance the anticancer activity. For example, IC_{50} value of Naproxen sodium salt on MCF7 and MDA-MB-231 cell lines are >5 mM and ~10 mM respectively [68]. There is no consensus in the literature regarding the molecular mechanism of the anticancer activity of NSAIDs. NAP is known to have anti-cancer activities against urinary bladder cancer and prostate cancer [23, 72]. Computer kinase profiling results suggested that phosphoinositide 3-kinase (PI3K) is a potential target for NAP in addition to cyclooxygenase (COX) that the NSAIDs are known to inhibit [73]. Naproxen also has significant inhibitory effect on human osteosarcoma cell line (MG-63), in a concentration-dependent manner [74].

Infact, toxicity of the nanodrugs can also occur due to a range of particle properties such as size, shape, charge and surface characteristics [69]. Lower particle size and surface characteristics may facilitate nanoparticles to penetrate into the cancer cell [69-71]. Zeta potential could be a reason for the oserved enhanced anti-leukaemia activity. This is because, raw-NAP as well as all the nanoformulated NSAIDs have similar zeta potentials whereas raw-IBP and raw-KP have more negative zeta potentials. Viability of Jurkat cells in presence of pure polymers was also screened and the results are presented in Figure S5 (electronic supporting information). No significant anti-leukaemia activity was observed even in presence of 80 µg/ml of the pure polymers. Thus, it can be concluded that NAP has significant anti-leukemia activity and the activity can be enhanced by nanoformulation, especially by using HPMC and PVP as polymeric stabilizers. Further studies are required to assess the actual mechanism of the observed enhanced anti-leukemia activity of the nanoformulated NAP samples.

4. Conclusions

EASAI method offers a greater control on particle size and morphology of drug nanoparticles including NSAIDs. Ultrafine nanoparticles of NSAIDs with size less than 30 nm could be prepared using EASAI method. The polymeric stabilizers effectively control the particle size even without strongly interacting with the drug. The reduction of particles size and the presence of the lyophilic polymers led to considerable enhancement in solubility and drug release rate. The particle size reduction by using EASAI does not result in any significant loss of crystallinity. NAP has significant anti-leukemia activity and this activity can further be enhanced using nanoformulation. Even though, IBP and KP do not have very high anti-leukemia activities when compared doxorubicin, nanoformulation resulted in enhancement of their anticancer activities also. In fact drug repositioning, i.e. finding new therapeutic activity of approved drugs can save a lot of cost and time that is involved in the development of new drug candidates for cancer therapy. The present concept of improving the anticancer activity by decreasing the particle size of poorly water soluble NSAIDs thus could open up new directions in anticancer drug development.

Acknowledgement

Thanks are due to Advanced Materials Research Centre (AMRC), IIT Mandi for providing laboratory facilities. Financial assistance from DRDO New Delhi (ARMREB/CDSW/2012/149) and UGC (SRF) to R. Kumar is gratefully acknowledged. Authors also thanked to ACTREC, Mumbai for conducting in-vitro anticancer screening.

References

[1] J. Jadhav, A. Juvekar, R. Kurane, S. Khanapure, R. Salunkhe, G. Rashinkar, Remarkable anti-breast cancer activity of ferrocene tagged multi-functionalized 1, 4-dihydropyrimidines, Eur. J Med. Chem. 65 (2013) 232-239.

[2] T. Mizushima, Molecular mechanism for various pharmacological activities of NSAIDS, Pharmaceuticals. 3 (2010) 1614-1636.

[3] M. Van Tulder, R. Scholten, B. Koes, R. Deyo, Non-steroidal anti-inflammatory drugs for low back pain, Cochrane. Database. Syst. Rev. 2 (2000) CD000396.

[4] R.D. Mann, The ancient world, Modern drug use: an enquiry on historical principles, Springer, Netharland. 1984, 1-58.

[5] H. Levesque, O. Lafont, Aspirin throughout the ages: a historical review, Rev. Med. Interne. 21 (2000) 8-17.

[6] K. Rainsford, History and development of the salicylates, Aspirin and related drugs. 2004, 1-23.

[7] S. Ferreira, S. Moncada, J. Vane, Prostaglandins and the mechanism of analgesia produced by aspirin-like drugs, Br. J. Pharmacol. 120 (1997) 401-412.

[8] R.A. Fryer, C. Galustian, A.G. Dalgelish, Recent advances and developments in treatment strategies against pancreatic cancer, Curr. Clin. Pharmacol. 4 (2009) 102-112.

[9] R.A. Gupta, R.N. DuBois, Colorectal cancer prevention and treatment by inhibition of cyclooxygenase-2, Nat. Rev. Cancer. 1 (2001) 11-21.

[10] R.E. Harris, R.T. Chlebowski, R.D. Jackson, D.J. Frid, J.L. Ascenseo, G. Anderson, A. Loar, R.J. Rodabough, E. White, A. McTiernan, Breast cancer and nonsteroidal anti-inflammatory drugs prospective results from the women's health initiative, Cancer Res. 63 (2003) 6096-6101.

[11] L.A.G. Rodríguez, C. Huerta-Alvarez, Reduced risk of colorectal cancer among long-term users of aspirin and nonaspirin nonsteroidal antiinflammatory drugs, Epidem. 12 (2001) 88-93.

[12] D.M. Schreinemachers, R.B. Everson, Aspirin use and lung, colon, and breast cancer incidence in a prospective study, Epidem. 5 (1994) 138-146.

[13] S.M. Sondhi, R. Rani, J. Singh, P. Roy, S. Agrawal, A. Saxena, Solvent free synthesis, anti-inflammatory and anticancer activity evaluation of tricyclic and tetracyclic benzimidazole derivatives, Bioorg. Med. Chem. Lett. 20 (2010) 2306-2310.

[14] M.S. Shaik, A. Chatterjee, T. Jackson, M. Singh, Enhancement of antitumor activity of docetaxel by celecoxib in lung tumors, Int. J. Cancer. 118 (2006) 396-404.

[15] D. Plano, D. N. Karelia, M. K. Pandey, J. E. Spallholz, S. Amin, A. K. Sharma. Design, synthesis and biological evaluation of novel Selenium (SeNSAID) molecules as anticancer agents, J. Med. Chem. 59 (2016) 1946−1959.
[16] E. Beetge, J. du Plessis, D.G. Müller, C. Goosen, F.J. van Rensburg, The influence of the physicochemical characteristics and pharmacokinetic properties of selected NSAID's on their transdermal absorption, Int. J. Pharm. 193 (2000) 261-264.
[17] P. Conte, V. Guarneri, Safety of intravenous and oral bisphosphonates and compliance with dosing regimens, The Oncologist. 9 (2004) 28-37.
[18] M.J. Thun, S.J. Henley, C. Patrono, Nonsteroidal anti-inflammatory drugs as anticancer agents: mechanistic, pharmacologic and clinical issues, J. Natl. Cancer Inst. 94 (2002) 252-266.
[19] M. Szkudliński, A proposed mechanism of anticancer activity of indomethacin, Med. Hypotheses. 39 (1992) 265-266.
[20] S. Hashitani, M. Urade, N. Nishimura, T. Maeda, K. Takaoka, K. Noguchi, K. Sakurai, Apoptosis induction and enhancement of cytotoxicity of anticancer drugs by celecoxib, a selective cyclooxygenase-2 inhibitor, in human head and neck carcinoma cell lines, Int. J. Oncol. 23 (2003) 665-672.
[21] F. Khwaja, J. Allen, J. Lynch, P. Andrews, D. Djakiew, Ibuprofen inhibits survival of bladder cancer cells by induced expression of the p75NTR tumor suppressor protein, Cancer. Res. 64 (2004) 6207-6213.
[22] V. Pace, Use of nonsteroidal anti-inflammatory drugs in cancer, Palliative Med. 9 (1995) 273-286.
[23] S. Srinivas, D. Feldman, A phase II trial of calcitriol and naproxen in recurrent prostate cancer, Anticancer Res. 29 (2009) 3605-3610.
[24] K. Adibkia, M. Barzegar-Jalali, A. Nokhodchi, M. Siahi Shadbad, Y. Omidi, Y. Javadzadeh, G. Mohammadi, A review on the methods of preparation of pharmaceutical nanoparticles, Pharm. Sci. 15 (2009) 303-314.
[25] J.G. Marques, V.M. Gaspar, E. Costa, C.M. Paquete, I.J. Correia, Synthesis and characterization of micelles as carriers of non-steroidal anti-inflammatory drugs (NSAID) for application in breast cancer therapy, Colloids Surf., B. 113 (2014) 375-383.
[26] P. Venkatesan, N. Puvvada, R. Dash, B.P. Kumar, D. Sarkar, B. Azab, A. Pathak, S.C. Kundu, P.B. Fisher, M. Mandal, The potential of celecoxib-loaded hydroxyapatite-chitosan nanocomposite for the treatment of colon cancer, Biomaterials. 32 (2011) 3794-3806.
[27] E.F. Da Silveira, J.M. Chassot, F.C. Teixeira, J.H. Azambuja, G. Debom, F.T. Beira, F.A. Del Pino, A. Lourenço, A.P. Horn, L. Cruz, Ketoprofen-loaded polymeric nanocapsules selectively inhibit cancer cell growth in vitro and in preclinical model of glioblastoma multiforme, Invest. New Drugs. 31 (2013) 1424-1435.
[28] P. Bonelli, F. Tuccillo, A. Federico, M. Napolitano, A. Borrelli, D. Melisi, M. Rimoli, R. Palaia, C. Arra, F. Carinci, Ibuprofen delivered by poly (lactic-co-glycolic acid)(PLGA) nanoparticles to human gastric cancer cells exerts antiproliferative activity at very low concentrations, Int. J. Nanomed. 7 (2012) 5683.

[29] E. Merisko-Liversidge, G.G. Liversidge, E.R. Cooper, Nanosizing: a formulation approach for poorly-water-soluble compounds, Eur. J. Pharm. Sci. 18 (2003) 113-120.
[30] J. Kipp, The role of solid nanoparticle technology in the parenteral delivery of poorly water-soluble drugs, Int. J. Pharm. 284 (2004) 109-122.
[31] H. Chen, C. Khemtong, X. Yang, X. Chang, J. Gao, Nanonization strategies for poorly water-soluble drugs, Drug Discovery Today. 16 (2011) 354-360.
[32] P. Kocbek, S. Baumgartner, J. Kristl, Preparation and evaluation of nanosuspensions for enhancing the dissolution of poorly soluble drugs, Int. J. Pharm. 312 (2006) 179-186.
[33] F. Kesisoglou, S. Panmai, Y. Wu, Nanosizing-oral formulation development and biopharmaceutical evaluation, Adv. Drug. Del. Rev. 59 (2007) 631-644.
[34] A. Singh, Z.A. Worku, G. Van den Mooter, Oral formulation strategies to improve solubility of poorly water-soluble drugs, Expert Opinio. Drug Del. 8 (2011) 1361-1378.
[35] A.N. Lukyanov, V.P. Torchilin, Micelles from lipid derivatives of water-soluble polymers as delivery systems for poorly soluble drugs, Adv. Drug. Del. Rev. 56 (2004) 1273-1289.
[36] R. Kumar, P.F. Siril, Ultrafine carbamazepine nanoparticles with enhanced water solubility and rate of dissolution, RSC Adv. 4 (2014) 48101-48108.
[37] D. Sharma, M. Soni, S. Kumar, G.D. Gupta, Solubility enhancement-eminent role in poorly soluble drugs, Res. J. Pharm. Technol. 2 (2009).
[38] F. Baines, N. Billingham, S. Armes, Synthesis and solution properties of water-soluble hydrophilic-hydrophobic block copolymers, Macromolecules. 29 (1996) 3416-3420.
[39] V.G. Kadajji, G.V. Betageri, Water soluble polymers for pharmaceutical applications, Polymers. 3 (2011) 1972-2009.
[40] S.R. Van Tomme, G. Storm, W.E. Hennink, In situ gelling hydrogels for pharmaceutical and biomedical applications, Int. J. Pharm. 355 (2008) 1-18.
[41] B.-J. Lee, S.-G. Ryu, J.-H. Cui, Controlled release of dual drug-loaded hydroxypropyl methylcellulose matrix tablet using drug-containing polymeric coatings, Int. J. Pharm. 188 (1999) 71-80.
[42] V. Caron, C. Bhugra, M.J. Pikal, Prediction of onset of crystallization in amorphous pharmaceutical systems: phenobarbital, nifedipine/PVP, and phenobarbital/PVP, J. Pharm. Sci. 99 (2010) 3887-3900.
[43] R.K. Gangwar, V.A. Dhumale, D. Kumari, U.T. Nakate, S. Gosavi, R.B. Sharma, S. Kale, S. Datar, Conjugation of curcumin with PVP capped gold nanoparticles for improving bioavailability, Mater. Sci. Eng. C. 32 (2012) 2659-2663.
[44] X.Y. Li, D.G. Yu, F.P. Jiang, K.J. Deng, Z. Du, X. Wang, Drug sustained release multiple-component polymeric microparticles fabricated using an electrospray process, Adv. Mater. Res. 2014, 269-275.
[45] B. Wan, S. Liao, D. Yu, Polymer-supported palladium–manganese bimetallic catalyst for the oxidative carbonylation of amines to carbamate esters, Appl. Catal., A. 183 (1999) 81-84.
[46] Q. Liu, R. Li, Z. Zhu, X. Qian, W. Guan, L. Yu, M. Yang, X. Jiang, B. Liu, Enhanced antitumor efficacy, biodistribution and penetration of docetaxel-loaded biodegradable nanoparticles, Int. J. Pharm. 430 (2012) 350-358.

[47] M.N. Patil, G.M. Gore, A.B. Pandit, Ultrasonically controlled particle size distribution of explosives: A safe method, Ultrason. Sonochem. 15 (2008) 177-187.
[48] P. Skehan, R. Storeng, D. Scudiero, A. Monks, J. McMahon, D. Vistica, J.T. Warren, H. Bokesch, S. Kenney, M.R. Boyd, New colorimetric cytotoxicity assay for anticancer-drug screening, J. Natl. Cancer Inst. 82 (1990) 1107-1112.
[49] V. Vichai, K. Kirtikara, Sulforhodamine B colorimetric assay for cytotoxicity screening, Nature protocol. 1 (2006) 1112-1116.
[50] S.M. Shah, P.N. Goel, A.S. Jain, P.O. Pathak, S.G. Padhye, S. Govindarajan, S.S. Ghosh, P.R. Chaudhari, R.P. Gude, V. Gopal, Liposomes for targeting hepatocellular carcinoma: Use of conjugated arabinogalactan as targeting ligand, Int. J. Pharm. 477 (2014) 128-139.
[51] H. Shete, S. Chatterjee, A. De, V. Patravale, Long chain lipid based tamoxifen NLC. Part II: Pharmacokinetic, biodistribution and in vitro anticancer efficacy studies, Int. J. Pharm. 454 (2013) 584-592.
[52] B. Sinha, R.H. Müller, J.P. Möschwitzer, Bottom-up approaches for preparing drug nanocrystals: formulations and factors affecting particle size, Int. J. Pharm. 453 (2013) 126-141.
[53] R. Kumar, P.F. Siril, P. Soni, Preparation of nano-RDX by evaporation assisted solvent-antisolvent interaction, Propellants, Explos., Pyrotech. 39 (2014) 383-389.
[54] R. Kumar, P.F. Siril, Controlling the size and morphology of griseofulvin nanoparticles using polymeric stabilizers by evaporation-assisted solvent–antisolvent interaction method, J. Nanopart. Res. 17 (2015) 1-11.
[55] S.V. Dalvi, R.N. Dave, Controlling particle size of a poorly water-soluble drug using ultrasound and stabilizers in antisolvent precipitation, Ind. Eng. Chem. Res. 48 (2009) 7581-7593.
[56] H. Dou, K.-H. Kim, B.-C. Lee, J. Choe, H.-S. Kim, S. Lee, Preparation and characterization of cyclo-1, 3, 5-trimethylene-2, 4, 6-trinitramine (RDX) powder: comparison of microscopy, dynamic light scattering and field-flow fractionation for size characterization, Powder Technol. 235 (2013) 814-822.
[57] R.S. Dhumal, S.V. Biradar, S. Yamamura, A.R. Paradkar, P. York, Preparation of amorphous cefuroxime axetil nanoparticles by sonoprecipitation for enhancement of bioavailability, Eur. J. Pharm. Biopharm. 70 (2008) 109-115.
[58] Z. Guo, X.-M. Liu, L. Ma, J. Li, H. Zhang, Y.-P. Gao, Y. Yuan, Effects of particle morphology, pore size and surface coating of mesoporous silica on Naproxen dissolution rate enhancement, Colloids Surf., B. 101 (2013) 228-235.
[59] M. Imran ul-haq, E. Chasovskikh, R. Signorell, Phase behavior of ketoprofen− poly (lactic acid) drug particles formed by rapid expansion of supercritical solutions, Langmuir. 26 (2010) 14951-14957.
[60] S. Plakkot, M. De Matas, P. York, M. Saunders, B. Sulaiman, Comminution of ibuprofen to produce nano-particles for rapid dissolution, Int. J. Pharm. 415 (2011) 307-314.

[61] M. Dixit, P.K. Kulkarni, V. Gowtham, H. Shivakumar, Preparation and Characterization of spray dried microparticle and chilled spray dried particle of Ketoprofen by spray drying method, Asian J. Pharm. Clin. Res. 4 (2011).
[62] K. Adibkia, Y. Javadzadeh, S. Dastmalchi, G. Mohammadi, F.K. Niri, M. Alaei-Beirami, Naproxen–Eudragit® RS100 nanoparticles: preparation and physicochemical characterization, Colloids Surf., B. 83 (2011) 155-159.
[63] S. Kheradmandnia, E. Vasheghani-Farahani, M. Nosrati, F. Atyabi, Preparation and characterization of ketoprofen-loaded solid lipid nanoparticles made from beeswax and carnauba wax, Nanomed. Nanotech. Biol. Med. 6 (2010) 753-759.
[64] D.G. Yu, X.F. Zhang, X.X. Shen, C. Brandford-White, L.M. Zhu, Ultrafine ibuprofen-loaded polyvinylpyrrolidone fiber mats using electrospinning, Polym. Int. 58 (2009) 1010-1013.
[65] N. Terzioglu, A. Gürsoy, Synthesis and anticancer evaluation of some new hydrazone derivatives of 2, 6-dimethylimidazo [2, 1-b][1, 3, 4] thiadiazole-5-carbohydrazide, Eur. J. Med. Chem. 38 (2003) 781-786.
[66] T. Aboul-Fadl, S.S. Al-Hamad, K. Lee, N. Li, B.D. Gary, A.B. Keeton, G.A. Piazza, M.K. Abdel-Hamid, Novel non-cyclooxygenase inhibitory derivatives of naproxen for colorectal cancer chemoprevention, Med. Chem. Res. 23 (2014) 4177-4188.
[67] T.M. Motawi, Y. Bustanji, S. EL-Maraghy, M.O. Taha, M.A. Al-Ghussein, Evaluation of naproxen and cromolyn activities against cancer cells viability, proliferation, apoptosis, p53 and gene expression of survivin and caspase-3, J. Enzyme Inhibit. Med. Chem. 29 (2014) 153-161.
[68] J. Deb, J. Majumder, S. Bhattacharyya, S.S. Jana, A novel naproxen derivative capable of displaying anti-cancer and anti-migratory properties against human breast cancer cells, BMC cancer. 14 (2014) 1.
[69] A. Verma, F. Stellacci, Effect of surface properties on nanoparticle–cell interactions, Small. 6 (2010) 12-21.
[70] A. Verma, O. Uzun, Y. Hu, Y. Hu, H.-S. Han, N. Watson, S. Chen, D.J. Irvine, F. Stellacci, Surface-structure-regulated cell-membrane penetration by monolayer-protected nanoparticles, Nat. Mater. 7 (2008) 588-595.
[71] M.E. Davis, D.M. Shin, Nanoparticle therapeutics: an emerging treatment modality for cancer, Nat. Rev. Drug Discov. 7 (2008) 771-782.
[72] R.A. Lubet, J.M. Scheiman, A. Bode, J. White, L. Minasian, M.M. Juliana, D.L. Boring, V.E. Steele, C.J. Grubbs, Prevention of chemically induced urinary bladder cancers by naproxen: protocols to reduce gastric toxicity in humans do not alter preventive efficacy, Cancer Prev. Res. 8 (2015) 296-302.
[73] M.-S. Kim, J.-E. Kim, Z. Huang, H. Chen, A. Langfald, R.A. Lubet, C.J. Grubbs, Z. Dong, A.M. Bode, Naproxen induces cell-cycle arrest and apoptosis in human urinary bladder cancer cell lines and chemically induced cancers by targeting PI3K, Cancer Prev. Res. 7 (2014) 236-245.
[74] I. Correia, R. Arantes-Rodrigues, R. Pinto-Leite, I. Gaivão, Effects of naproxen on cell proliferation and genotoxicity in MG-63 osteosarcoma cell line, J. Toxicol. Environ. Health. A. 77 (2014) 916-923.

Caption of figures

Figure 1 Schematic representation of the mechanism of nanoparticle formation in the EASAI method.

Figure 2 Representative FESEM images of the nanoparticles of IBP.

Figure 3 Representative FESEM images of the nanoparticles of KP.

Figure 4 Representative FESEM images of the nanoparticles of NAP.

Figure 5 In-vitro drug release profiles of raw-NSAIDs and their nanoformulated samples.

Figure 6 Plots of % cell viability of human leukemia cells (Jurkat) against varying concentrations of raw and nanoformulated NSAIDs. Average particle size of the nanoformulated NSAIDs that were measured from FESEM images are mentioned along with respective samples.